Long-range Josephson coupling through ferromagnetic graphene

Ali G. Moghaddam and Malek Zareyan
Institute for Advanced Studies in Basic Sciences (IASBS), P.O. Box 45195-1159, Zanjan 45195, Iran
(Received 22 June 2008; revised manuscript received 11 August 2008; published 15 September 2008)

We study the Josephson effect in graphene-based ballistic superconductor-ferromagnet-superconductor (SFS) junctions. We find an oscillatory Josephson coupling I_cR_N of F graphene whose amplitude is nonvanishing for a half-metallic graphene, increases for the exchange fields h above the Fermi energy E_F and shows only a slow damping at strong exchange fields $h \gg E_F$. We interpret this long-range Josephson coupling as the result of the exchange mediated Andreev-Klein process at FS interfaces which enhances the induced antiparallel-spin superconducting correlations in F graphene by increasing h above E_F. We further demonstrate the existence of regular temperature-induced transitions between 0 and π couplings in the plane of T and h where the phase boundaries have distinct shapes at the two regimes of h below and above E_F.

DOI: 10.1103/PhysRevB.78.115413 PACS number(s): 73.23.−b, 85.75.−d, 74.45.+c, 74.78.Na

I. INTRODUCTION

Graphene, the two-dimensional (2D) solid of carbon atoms with honeycomb lattice structure, shows unique properties due to its peculiar gapless semiconducting band structure.[1–4] The conduction and valence bands in graphene have the conical form at low energies with the apexes of the cones touching each other at the corners of the hexagonal first Brillouin zone which determine two nonequivalent valleys in the band structure. The charge-carrier type [electronlike (n) or holelike (p)] and its density can be tuned by means of electrical gates or doping of underlying substrate. An important aspect in graphene is the connection between its specific band structure and the pseudospin which characterizes the relative amplitude of electron wave function in two distinct trigonal sublattices of the hexagonal structure. This has caused the charge carriers in graphene to behave as 2D massless Dirac fermions with a pseudo-relativistic *chiral* property.[1] Already anomalies of a variety of phenomena including quantum Hall effect,[1] Andreev reflection (AR),[5,6] and Josephson effect[7,8] in graphene have been demonstrated. Here we report on the peculiarity of Josephson effect in a graphene superconductor-ferromagnet-superconductor (SFS) junction, which arises from such a Dirac-type spectrum with chirality. We find that a weakly doped graphene F contact can support a long-ranged *opposite-spin* supercurrent which persists at strong spin-splitting exchange fields, in striking contrast to the behavior of the Josephson current in common SFS junctions.[9]

Superconducting correlations can propagate through a mesoscopic normal-metal (N) contact between two superconductors (S) via the process of AR at the NS interfaces in which the subgap electron and hole excitations with opposite spin directions are converted to each other.[10] Successive AR at the two NS interfaces and the coherent propagation of the excitations between these reflections lead to the formation of the so-called Andreev bound states which can carry a supercurrent. The resulting Josephson effect, characterized by the critical (maximum) supercurrent I_c and a relation with the phase difference φ between superconducting order parameters of the two superconductors, is well established in a variety of SNS structures.[11] In an SFS junction, due to the exchange correlations field h, a momentum change of $2h/v_F$ between Andreev correlated electron holes is induced which results in a damped oscillatory variation of I_c with the length of F-contact L. As the result of the I_c oscillations a SFS structure can transform into the so-called π junction in which the ground-state phase difference between two superconductors is π instead of 0.[9,12] The damping of I_c occurs over the magnetic coherence length ξ_h which is $\sim \hbar v_F/h$ for a ballistic F.[13,14] This makes the Josephson coupling in F junctions rather short ranged as compared to SNS systems in which the Josephson coupling persists over much longer lengths of order of the normal-metal coherence length $\xi_N = \hbar v_F/k_BT$ (Ref. 9) (normally h is much larger than the superconducting gap Δ). In particular for a half-metal F contact with $h \geq E_F$ there is no Josephson coupling for a sizable contact of length $L \gtrsim \lambda_F$.[14]

In this work, we demonstrate unusual features of the exchange-induced I_c oscillations and the corresponding $0-\pi$ transitions in a ballistic F-graphene Josephson contact between two highly doped superconducting regions (see Fig. 1). We show that while in the regime of $h < E_F$ the amplitude of the critical current shows a monotonic damping with the exchange field, for the higher exchange fields $h \geq E_F$ it develops drastically different behavior. For a half-metal F with $h = E_F$, we find that the Josephson coupling I_cR_N (R_N being the normal-state resistance of the junction) has a *nonvanishing* value, in spite of the vanishing density of states for spin-down electrons. Interestingly, this finite Josephson coupling resulted from particular Andreev bound states in which spin-up propagating excitations and spin-down *evanescent* excitations are involved. These mixed evanescent-propagating states can have significant contribution in the supercurrent due to the chiral nature of the carriers in F graphene.[7,15]

More surprisingly, we find that for exchange fields above the Fermi energy $h \gtrsim E_F$ the coupling I_cR_N *increases* above its half-metal value and shows damping only at strong exchange fields $h \gg E_F$ with a rate which is much lower than that of the regime of $h < E_F$. We explain this long-range Josephson effect in terms of superconducting correlations between a n-type excitation from the spin-up conduction subband and a p-type excitation from the spin-down valence subband in F [see Fig. 1(b)]. For $h > E_F$ these two types of

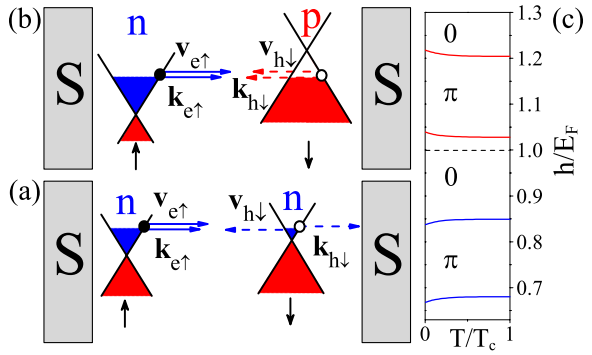

FIG. 1. (Color online) (a)–(b) Schematic of the graphene SFS junction and the configuration [being electronlike (n) and holelike (p)] of the spin-up and spin-down subbands for two regimes of (a) $h<E_F$ and (b) $h>E_F$. The orientation of the wave vectors and velocity vectors of Andreev correlated electron holes (moving perpendicular to the interfaces) is also shown. For $h<E_F$ the retro reflected hole has antiparallel momentum and velocity, whereas for $h>E_F$ Andreev reflection is specular with the hole having parallel momentum and velocity. (c) Phase diagram of the $0-\pi$ transition of the junction of $E_FL/\hbar v_F=10$ around $h=E_F$. The boundaries between 0 and π phases for $h>E_F$ and $h<E_F$ are the mirror form of each other.

excitations are coupled at the FS interfaces via a peculiar Andreev process which is accompanied by a Klein tunneling through the exchange field $p-n$ barrier.[16] It has been found that this spin Andreev-Klein process leads to an enhancement of the amplitude of AR and the resulting subgap conductance of FS junctions with the exchange field. In the SFS structure the corresponding Andreev-Klein bound states are responsible for the long-range proximity effect. We further demonstrate the existence of the temperature-induced regular $0-\pi$ transitions by presenting phase diagram in T/T_c and h/E_F plane where the boundaries of $0-\pi$ phases have different forms in two regimes of $h<E_F$ and $h>E_F$.

II. MODEL AND BASIC EQUATIONS

To be specific, we consider a ballistic F-graphene strip of length L smaller than the superconducting coherence length $\xi=\hbar v_F/\Delta$ which connects two S electrodes (see Fig. 1). Highly doped superconducting regions can be produced by depositing superconducting metallic electrodes on top of the graphene sheet.[8] A graphene SFS structure similar to our setup has been studied by Linder *et al.*[17] considering certain values for the Fermi energy in F and in the electrodes. They concentrated on the existence of a large residual supercurrent in the points of $0-\pi$ transitions at $T=0$. Here we consider a more realistic model of highly doped S electrodes and cover full range of the key parameter h/E_F to find the above-mentioned long-range Josephson coupling whose underlying mechanism will be explained in the following. We take the Fermi wavelength λ_{FS} of S electrodes to be much smaller than the superconducting coherence length ξ and the Fermi wavelength in F-graphene λ_F ($E_{FS}\gg E_F, \Delta$). By the first condition mean-field theory of superconductivity will be justified and by the second we can neglect the spatial variation of the superconducting order parameter $\Delta(x)$ in the superconductors close to the FS interfaces. Thus $\Delta(x)$ has the constant values $\Delta\exp(\pm i\varphi/2)$ in the left and right superconductors, respectively, and vanishes identically in F.

The superconducting correlations between a spin σ electron excitation of wave function u_σ and the spin $\bar{\sigma}$ hole excitation of wave function $v_{\bar{\sigma}}$ can be described by Dirac–Bogoliubov–de Gennes (DBdG)[5] equation which, in the presence of an exchange field, reads

$$\begin{pmatrix} \hat{H}_\sigma - E_F - \varepsilon & \hat{\Delta} \\ \hat{\Delta}^* & E_F - \hat{H}_{\bar{\sigma}} - \varepsilon \end{pmatrix} \begin{pmatrix} u_\sigma \\ v_{\bar{\sigma}} \end{pmatrix} = 0. \tag{1}$$

Here $\hat{H}_\sigma=-i\hbar v_F(\partial_x\hat{\sigma}_x+\partial_y\hat{\sigma}_y)-\sigma h$ and $\hat{\Delta}=\Delta\hat{\sigma}_0$ are the spin-σ single-electron Dirac Hamiltonian and the superconducting pair potential, respectively, and ε is the excitation energy. The wave functions u_σ and $v_{\bar{\sigma}}$ are two-component spinors of the form (ψ_1,ψ_2) and $\hat{\sigma}_i$ $(i=0,x,y,z)$ are Pauli matrices, all operating in the space of two sublattices (pseudospin) of the honeycomb lattice.

Inside F the solutions of DBdG Eq. (1) are electron and holelike wave functions which are classified by a 2D wave vector $\mathbf{k}_\sigma\equiv(k_\sigma,q)$ with the energy-momentum relation $\varepsilon_\sigma=\hbar v_F|\mathbf{k}_\sigma|$. For a finite width W the transverse momentum is quantized $[q_n=(n+1/2)\pi/W]$ by imposing the infinite mass boundary conditions at the edges.[18] At the Fermi level $\varepsilon=0$ for a spin direction σ and a given q_n there are two electron and two hole states with the wave functions

$$u_\sigma = v_\sigma = e^{\pm ik_\sigma x+iqy}(1, \pm e^{\pm i\alpha_\sigma}), \tag{2}$$

which are characterized by longitudinal momentum $k_\sigma=\sqrt{k_{F\sigma}^2-q^2}$ and the propagation angle $\alpha_\sigma=\arcsin(q/k_{F\sigma})$ $[k_{F\sigma}=(E_F+\sigma h)/(\hbar v_F)$ being the Fermi wave vector of spin σ subband].

The solutions of Eq. (1) inside S ($h=0$) are rather mixed electron-hole excitations, the so-called Dirac-Bogoliubov quasiparticles. Assuming ideal FS contacts the electron-hole conversion can be described by a boundary condition between electron and hole wave functions which for the left and right interfaces, respectively, has the forms[7]

$$u_\sigma = e^{\mp i\varphi/2+i\beta\mathbf{n}\cdot\boldsymbol{\sigma}}\, v_{\bar{\sigma}}, \quad \beta=\arccos(\varepsilon/\Delta), \tag{3}$$

where $\mathbf{n}$ is the unit vector perpendicular to a FS interface pointing from F to S.

Introducing the normal-state transmission coefficient of spin σ quasiparticles through the junction as

$$t_\sigma = |t_\sigma|e^{i\eta_\sigma} = \frac{1}{\cos\gamma_\sigma - i\sin\gamma_\sigma/\cos\alpha_\sigma}, \tag{4}$$

with $\gamma_\sigma=k_\sigma L$ and imposing conditions (3) at the two FS boundaries ($x=0,L$), we obtain the following result for the energy of the spin σ Andreev bound state:

$$\varepsilon_\sigma = \Delta\cos\{[\theta(\varphi)+\eta_{\bar{\sigma}}-\eta_\sigma]/2\}, \tag{5}$$

where $\cos\theta=|t_\sigma t_{\bar{\sigma}}|[\cos\varphi+\tan\alpha_\sigma\tan\alpha_{\bar{\sigma}}\sin\gamma_\sigma\sin\gamma_{\bar{\sigma}}]$. For a short junction of $L\ll\xi$ only the Andreev bound states with energies $|\varepsilon|<\Delta_0$ have the main contribution to the supercur-

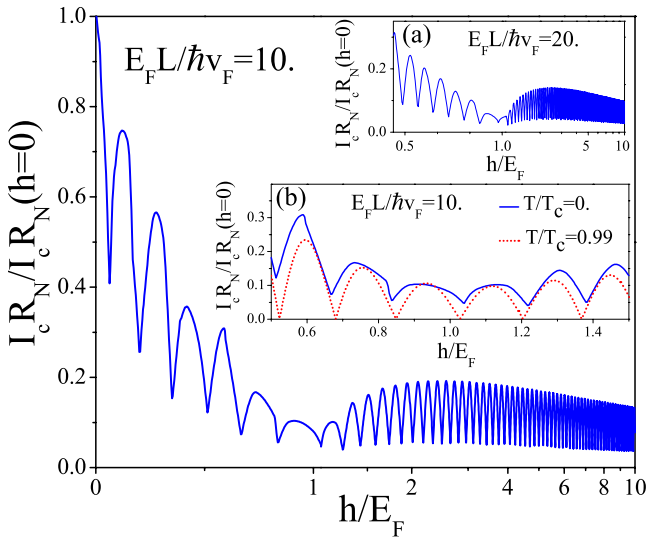

FIG. 2. (Color online) Dependence of the zero-temperature Josephson coupling I_cR_N on the exchange energy h/E_F for the length $E_FL/\hbar v_F=10$. Cusplike variations indicate $0-\pi$ transitions with a period $\simeq hL/\hbar v_F$. The coupling has a nonzero value for $h/E_F=1$, develops a smooth maximum for $h/E_F \gtrsim 1$ and shows a slow damping at strong exchange fields. For $h/E_F>1$ the scale of h/E_F is logarithmic. Inset (a) shows the same plot for a different length $E_FL/\hbar v_F=20$ to indicate that the appearance of maximum and slow decay are generic properties of the graphene SFS structure. Inset (b) shows the variations of I_cR_N with h/E_F at different temperatures $T=0$ (solid line) and $T=0.99T_c$ (dotted line).

rent. At temperature T the Josephson current can be obtained from the formula[19]

$$I = -\frac{2e}{\hbar}\sum_{n,\sigma} \tanh(\varepsilon_{\sigma,n}/2k_BT)\frac{d\varepsilon_{\sigma,n}}{d\varphi}, \tag{6}$$

where the factor 2 accounts for the valley degeneracy.

In general for arbitrary temperatures there is no simple analytic relation for the supercurrent from the above formula. However, near the critical temperature T_c, we can proceed analytically by using the fact that $\Delta(T \simeq T_c) \ll k_BT_c$. Then we obtain from Eq. (6) the following relation for the Josephson current:

$$I = \frac{e\Delta^2}{2\hbar k_BT_c}\sin\varphi \sum_n \Re(t_+t_-^*). \tag{7}$$

We see that near T_c the current-phase relation is sinusoidal, which is a common property of Josephson junctions.

III. RESULTS AND DISCUSSIONS

From Eq. (6) we have calculated the Josephson critical current. Figure 2 shows the dependence of resulting Josephson coupling I_cR_N on the exchange energy h/E_F scaled in units of Fermi energy at zero temperature and for $E_FL/\hbar v_F=10$. Here $R_N=(e^2/\pi\hbar\Sigma_{n,\sigma}|t_\sigma|^2)^{-1}$ is the resistance of the corresponding normal (nonsuperconducting) structure. Note that R_N decreases monotonically with the exchange field for $h>E_F$, due to the linear increase in the density of states in both spin subbands. In spite of showing the regular cusp form variations indicating $0-\pi$ transitions for all h/E_F, the overall behavior of the coupling in the regimes of $h<E_F$ and $h>E_F$ is drastically different. For $h<E_F$ the envelope of the curve decreases monotonically with h/E_F to reach a minimum for a half-metallic graphene $h=E_F$, just similar to the behavior of I_cR_N in a common SFS junction.[14] However for $h \geq E_F$ the coupling has a finite value and surprisingly increases smoothly with h before showing a slow damping at strong exchange fields $h \gg E_F$. Thus I_cR_N as a function of h develops a smooth maximum at an exchange field which we have found to depend weakly on the doping of F graphene $E_FL/\hbar v_F$.

We can understand the above behavior of I_cR_N in terms of the change in the configuration of the two spin subbands by varying the ratio h/E_F. For a normally n-doped F graphene ($E_F>0$), while for $h<E_F$ the charge carriers in both spin subbands are of the same n type [Fig. 1(a)]; for $h>E_F$ the spin-down carriers turn into the p type as the Fermi level shifts into the valence subband [Fig. 1(b)]. For $h<E_F$ the Andreev bound states which carry the supercurrent are made of electrons and holes with the same type n as shown in Fig. 1(a). The AR of the excitations at the Fermi level is of retro type as in an ordinary FS interface. In this regime by increasing h/E_F the amplitude of AR decreases, which leads to a decline in the Josephson coupling of the SFS junction. However when $h>E_F$ Andreev correlated electron-hole pairs in F are of different n and p types which are coupled via a specular[5,16] AKR at FS interfaces. Due to the exchange field induced enhancement of the amplitude of AKR, the resulting Josephson coupling I_cR_N shows an increase by h for $h \gtrsim E_F$. But this increase does not continue for higher h/E_F where I_cR_N decreases very slowly after showing a smooth maximum. This slow decline of I_cR_N, in spite of the increase in the amplitude of AKR, is the result of the interference of the contributions of different transverse modes (have different phases in general) in I_c [see Eq. (6)].

It is worth noting that, in contrast to the Josephson coupling, the critical current increases monotonically for $h>E_F$ because of the increase in the density of states for both spin directions, and hence the normal-state conductance.[20] This is shown in Fig. 3 where $I_c(h)/I_c(0)$ is plotted versus h/E_F for $E_FL/\hbar v_F=10$. Here we concentrate mostly on the behavior of the Josephson coupling which represents the real strength of superconducting coupling and does not contain the above-mentioned normal-state effect.

The behavior of Josephson junction with a half-metal graphene $h=E_F$ in which the density of states of the down-spin subband goes to zero is even more dramatic. In spite of the fact that there is no propagating excitation at the Fermi level with down spin, we still find a nonzero critical current for $h=E_F$ as it is seen in Fig. 2. Indeed, in this case we have only Andreev bound states combined from propagating spin-up electrons (holes) and evanescent spin-down holes (electrons). Such Andreev states exist for all values of h/E_F, however their contribution to the supercurrent is negligible unless at the vicinity of $h=E_F$ where they play the main role.

Now let us analyze the effect of a finite temperature. From Eq. (6) we have found that the ballistic graphene SFS junction can transit from zero state to π state by varying the

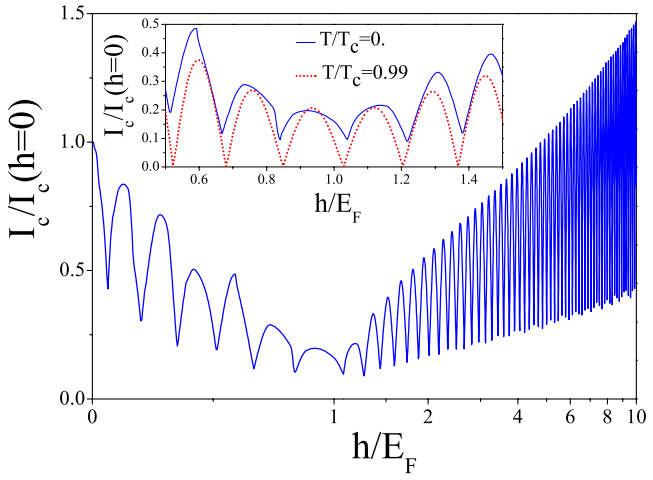

FIG. 3. (Color online) Dependence of the zero-temperature critical current I_c on the exchange energy h/E_F for the length $E_FL/\hbar v_F=10$. The critical current for $h<E_F$ decreases and after a minimum at $h=E_F$ begins to increase monotonically for $h>E_F$ due to the increase in the density of states. The inset compares the variations of I_c with h/E_F at $T=0$ (solid line) and $T=0.99T_c$ (dotted line). It shows that the places of $0-\pi$ cusps are different for different temperatures.

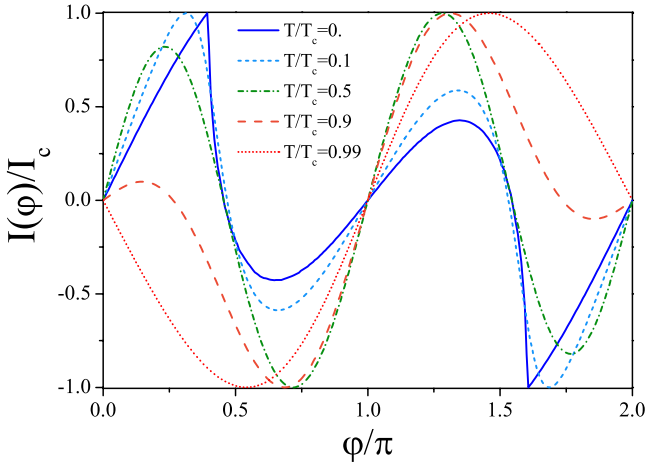

FIG. 4. (Color online) Current-phase relation of SFS junction at different temperatures for the length $E_FL/\hbar v_F=10$ and exchange energy $h/E_F=0.848$ (near sixth cusp in Fig. 3).

temperature. The resulting phase diagram in the plane of T/T_c and h/E_F is shown in Fig. 1(c) around $h=E_F$ and when $E_FL/\hbar v_F=10$. As it can be seen the values of exchange fields in which $0-\pi$ transitions occur increase (decrease) with temperature for the regime of $h<E_F$ ($h>E_F$) such that the phase boundaries for $h>E_F$ are the mirror form of those for $h<E_F$. This $0-\pi$ phase diagram is different from that of a common ballistic SFS junction.[21]

In ordinary ballistic SFS junctions the $0-\pi$ transition points remain unchanged with varying the temperature, unless there is a scattering region like an insulating barrier with small transparency. Indeed it has been shown that the width of the transitions, indicating the interval of the change field over which the temperature-induced $0-\pi$ transition is possible, increases by decreasing the transparency of the scattering region.[9,21] In our graphene SFS junction there is a normal scattering mechanism due to a large difference in the Fermi energies of S and F regions. Therefore the change in the $0-\pi$ transition points with temperature is expected. However we note that the width of the transition is quite small, as is seen in Fig. 1(c). The small width of the transition can be attributed to the chiral property of graphene and the associated Klein tunneling[5] due which an electron has an appreciable transmission probability through the interfaces despite the existence of the large potential steps.

The temperature-induced $0-\pi$ transition can also be seen from the inset of Fig. 3 where we have compared the oscillations of I_c at two temperatures $T=0$ and $T=0.99T_c$. We see that the place of a $0-\pi$ cusp depends on T. This dependence is different in two regimes of $h<E_F$ and $h>E_F$, which results in different forms of the phases boundaries as described above. The difference in the shape of phase boundaries for two regimes is an indication of difference between conventional Andreev bound states (in the regime of $h<E_F$) and Andreev-Klein bound states (in the regime of $h>E_F$). For $h<E_F$ the transition points decrease by decreasing the temperature which is a very general property of common SFS junctions.[9] But for $h>E_F$ the transition points increase when temperature is lowered. This difference with usual systems can be considered as a signature of Andreev-Klein bound states which exist only in graphene SFS structures for large exchange energies $h>E_F$.

As the final remark on the temperature dependence of the Josephson current, in Fig. 4 we show the current-phase relation for different temperatures and when $h/E_F=0.848$. This value of the exchange field corresponds to a point in the vicinity of the sixth cusp in the variation of I_cR_N in Fig. 3. It is clear that at low temperatures the current-phase relation is strongly nonsinusoidal which results in a large residual supercurrent at a transition point.[17] By increasing the temperature the contribution of higher harmonics in Josephson current decreases and as $T\rightarrow T_c$ the current-phase relation becomes pure sinusoidal (dotted line in Fig. 4). This limit corresponds to a vanishing supercurrent at the transition (inset of Fig. 3). As another point, the temperature-induced transition is also evident in Fig. 4. The junction is at zero state at low temperatures $T/T_c=0.,0.1$ and in the π state at higher temperatures $T=0.5,0.9,0.99$.

We note that the long-range Josephson coupling in graphene SFS junctions is carried by the superconducting correlations of two electrons with *opposite* spins. This effect, arising from the Dirac-type spectrum of excitations and their chiral nature, is fundamentally distinct from the recently discovered long-range proximity effect in ordinary SFS structures, which was attributed to the generation of the spin-parallel triplet correlations by inhomogeneity in the direction of the exchange field.[22]

The practical importance of the effects predicted here is connected with the possibility of fabricating high quality FS structures in graphene which seems to be quite feasible by considering the recent experimental realizations of proximity induced superconductivity[8,23] and ferromagnetic correlations[24–26] in graphene. In addition to proximity induced correlations,[27] intrinsic ferromagnetism were also predicted to exist in graphene sheets[28] and nanoribbons.[29] One

alternative way to produce Josephson F contact would be doping of the spacing part between two S regions (on top of which metallic superconducting electrodes are deposited) by magnetic atom impurities.[30]

IV. CONCLUSIONS

In conclusion, we have demonstrated the existence of a long-range supercurrent in weakly doped graphene ferromagnetic Josephson junctions. In contrast to the common view, a half-metallic graphene shows a nonvanishing Josephson coupling I_cR_N which increases by increasing the exchange field h above the Fermi energy E_F, and shows only a slow damping at strong exchanges $h \gg E_F$. We have explained this long-range coupling as the result of the exchange field mediated Andreev-Klein process at FS interfaces, which enhances the induction of superconducting correlations between electrons with opposite spins in F. We have also presented the $0-\pi$ phase diagram of the coupling in the plane of T/T_c and h/E_F, which reveals the distinct shapes of the phase boundaries in two cases of $h > E_F$ and $h < E_F$.

[1] K. S. Novoselov, A. K. Geim, S. V. Morozov, D. Jiang, M. I. Katsnelson, I. V. Grigorieva, S. V. Dubonos, and A. A. Firsov, Nature (London) **438**, 197 (2005); Y. Zhang, Y. W. Tan, H. L. Stormer, and P. Kim, *ibid.* **438**, 201 (2005).

[2] A. K. Geim and K. S. Novoselov, Nat. Mater. **6**, 183 (2007).

[3] M. I. Katsnelson and K. S. Novoselov, Solid State Commun. **143**, 3 (2007).

[4] A. H. Castro Neto, F. Guinea, N. M. R. Peres, K. S. Novoselov, and A. K. Geim, arXiv:0709.1163, Rev. Mod. Phys. (to be published).

[5] C. W. J. Beenakker, Phys. Rev. Lett. **97**, 067007 (2006).

[6] C. W. J. Beenakker, arXiv:0710.3848, Rev. Mod. Phys. (to be published).

[7] M. Titov and C. W. J. Beenakker, Phys. Rev. B **74**, 041401(R) (2006).

[8] H. B. Heersche, P. Jarillo-Herrero, J. B. Oostinga, L. M. K. Vandersypen, and A. F. Morpurgo, Nature (London) **446**, 56 (2007).

[9] A. I. Buzdin, Rev. Mod. Phys. **77**, 935 (2005).

[10] A. F. Andreev, Sov. Phys. JETP **19**, 1228 (1964).

[11] K. K. Likharev, Rev. Mod. Phys. **51**, 101 (1979).

[12] V. V. Ryazanov, V. A. Oboznov, A. Yu. Rusanov, A. V. Veretennikov, A. A. Golubov, and J. Aarts, Phys. Rev. Lett. **86**, 2427 (2001).

[13] A. I. Buzdin, L. N. Bulaevskii, and S. V. Panyukov, JETP Lett. **35**, 178 (1982).

[14] J. Cayssol and G. Montambaux, Phys. Rev. B **71**, 012507 (2005).

[15] A. G. Moghaddam and M. Zareyan, Phys. Rev. B **74**, 241403(R) (2006).

[16] M. Zareyan, H. Mohmmadpour, and A. G. Moghaddam, arXiv:0804.2774 (unpublished).

[17] J. Linder, T. Yokoyama, D. Huertas-Hernando, and A. Sudbo, Phys. Rev. Lett. **100**, 187004 (2008).

[18] M. V. Berry and R. J. Mondragon, Proc. R. Soc. London, Ser. A **412**, 53 (1987).

[19] C. W. J. Beenakker and H. van Houten, Phys. Rev. Lett. **66**, 3056 (1991).

[20] Y. Asano, T. Yoshida, Y. Tanaka, and A. A. Golubov, Phys. Rev. B **78**, 014514 (2008).

[21] N. M. Chtchelkatchev, W. Belzig, Yu. V. Nazarov, and C. Bruder, JETP Lett. **74**, 323 (2001).

[22] R. S. Keizer, S. T. B. Goennenwein, T. M. Klapwijk, G. Miao, G. Xiao, and A. Gupta, Nature (London) **439**, 825 (2006); F. S. Bergeret, A. F. Volkov, and K. B. Efetov, Phys. Rev. Lett. **86**, 4096 (2001); M. Eschrig and T. Löfwander, Nat. Phys. **4**, 138 (2008).

[23] A. Shailos, W. Nativel, A. Kasumov, C. Collet, M. Ferrier, S. Gueron, R. Deblock, and H. Bouchiat, Europhys. Lett. **79**, 57008 (2007).

[24] N. Tombros, C. Jozsa, M. Popinciuc, H. T. Jonkman, and B. J. van Wees, Nature (London) **448**, 571 (2007).

[25] E. W. Hill, A. K. Geim, K. Novoselov, F. Schedin, and P. Blake, IEEE Trans. Magn. **42**, 2694 (2006).

[26] C. Józsa, M. Popinciuc, N. Tombros, H. T. Jonkman, and B. J. van Wees, Phys. Rev. Lett. **100**, 236603 (2008).

[27] H. Haugen, D. Huertas-Hernando, and A. Brataas, Phys. Rev. B **77**, 115406 (2008); T. Yokoyama, *ibid.* **77**, 073413 (2008).

[28] N. M. R. Peres, F. Guinea, and A. H. Castro Neto, Phys. Rev. B **72**, 174406 (2005).

[29] Y.-W. Son, M. L. Cohen, and S. G. Louie, Nature (London) **444**, 347 (2006).

[30] V. K. Dugaev, V. I. Litvinov, and J. Barnas, Phys. Rev. B **74**, 224438 (2006); B. Uchoa, V. N. Kotov, N. M. R. Peres, and A. H. Castro Neto, Phys. Rev. Lett. **101**, 026805 (2008).